

Available online at www.sciencedirect.com

JOURNAL OF NON-CRYSTALLINE SOLIDS

Journal of Non-Crystalline Solids 334&335 (2004) 517-523

www.elsevier.com/locate/jnoncrysol

Laser cladding of quasicrystal forming Al-Cu-Fe on aluminum

Krishanu Biswas a, Rolf Galun b, Barry L. Mordike b, Kamanio Chattopadhyay a,*

^a Department of Metallurgy, Indian Institute of Science, Bangalore 560012, India ^b IWW, Technical University, Agricolasstrasse 6, D-38678 Clausthal-Zellerfeld, Germany

Abstract

Composite quasicrystalline coatings are developed by laser cladding of an elemental powder mixture of aluminum, copper and iron on an aluminum substrate. Some of the tracks are remelted to see the effect of phase formation and related changes in hardness during remelting. The clad layers start growing with a cellular morphology from the substrate. The icosahedral phase forms in all the tracks along with some aluminides. It has also been found that the icosahedral phase forms both by a peritectic reaction between the liquid and $Al_{13}Fe_4$ and by direct nucleation from the liquid. This is a clear indication of a different levels of undercooling that the liquid undergoes before the nucleation of the primary phase inside the clad layers during laser processing. The formation of $Al_{13}Fe_4$ with a ten-pointed star like morphology has also been found at the bottom of the clad. The remelting of the clad tracks leads to a change in microstructure as far as phase formation is concerned. The formation of long lath-shaped $Al_{13}Fe_4$ can be observed in the remelted layer. The hardness profiles of the clad and remelted layers reveal a hardness (HV_{0.025}) around 600.

© 2004 Published by Elsevier B.V.

PACS: 61.10.Eq; 61.16Bg; 61.14.Lj; 62.20.Qp

1. Introduction

Current research has demonstrated many desirable characteristics of quasicrystals such as high hardness [1], low friction coefficient [2], reasonable oxidation and corrosion resistance [3], low thermal and electrical conductivities [4] and unusual optical properties [5]. These materials have shown great potential for use in the fields of low friction and wear resistant coatings [6]. However, the use of the quasicrystalline material in the bulk form is difficult because of the brittleness that these materials exhibit at room temperature [7]. A possible alternative is to synthesize quasicrystalline coatings which exhibit the favorable properties of these materials. We have explored the potential of a laser cladding and alloying process to synthesize such a coating. This process is characterized by melting a powder mixture together with a thin layer of substrate using a scanning laser beam falling perpendicular to the substrate. This leads to the rapid solidification and the formation of the coating by

material build-up on the substrate. The laser cladding can be a single-step or two-step process. In the singlestep process, the material as a powder, wire or preplaced paste is injected into the melt pool created by the laser beam. In the case of the two-step laser cladding process, the coating materials in the form of powder, paste or wire are pre-deposited on the substrate and subsequently melted with the laser beam to form the coating. The pre-deposition of the coating can also be done by laser cladding. The microstructural evolution due to rapid solidification of the melt during the laser processing can lead to formation of a number of crystalline phases along with quasicrystalline phases. These crystalline phases include Al₁₃Fe₄ and CuAl₂, in addition to the aluminum solid solution. Al₁₃Fe₄ has monoclinic structure (a = 1.55 nm, b = 0.80721 nm, c = 1.2473 nm and $\beta = 107.731^{\circ}$), while CuAl₂ has a tetragonal structure (a = 0.6063 nm and c = 0.4872nm). It has been reported in the literature that a single region of Al₁₃Fe₄ extends from binary Al₁₃Fe₄ to the ternary space up to about 6 at.% Cu [8]. The formula of this phase can be written as (Al,Cu)₁₃Fe₄.

In this paper, we report the synthesis of a composite coating consisting of the icosahedral phase and aluminides using a two-step laser processing of the

^{*}Corresponding author. Tel.: +91-80 360 1991/309 2678/394 2678; fax: +91-80 360 1991/360 0683/360 1198.

E-mail address: kamanio@metalrg.iisc.ernet.in (K. Chattopadhyay).

quasicrystal-forming $Al_{65}Cu_{23.3}Fe_{11.7}$ powder on an aluminum substrate. In an earlier paper [9], Chattopadhyay et al. reported the formation of a composite quasicrystalline coating by laser cladding an elemental powder mixture of Al, Cu and Fe of $Al_{65}(Cu + Fe)_{35}$ with Cu/Fe = 2/1. The powder composition was adjusted accordingly in the present work in order to form quasicrystalline phases in the clad and remelted layers.

2. Experimental details

Clad layers were prepared using a continuous wave CO₂ laser (made by Rofin Sinar) with the following parameters:

Power 5 kW Beam diameter 5 mm

Focus 30 mm out of focus

Width of track 2 mm
Feed rate of powder 6 gm/min
Carrier gas (Ar) flow rate 4 l/min

The laser beam used was of a multimode configuration. An argon jet was used to shield the melt pool from oxygen. The substrates were moved under the stationary laser beam by a numerically controlled X–Y table. The nominal chemical composition of the powder mixture, Al₆₅Cu_{23.3}Fe_{11.7}, was obtained by mechanically mixing commercially pure elemental powder (99% minimum) of Al, Cu and Fe. The particle sizes of the powders were between 25 and 100 µm. The powder mixture was carried by an argon jet, through a nozzle with an inner diameter of 2 mm and delivered to the melt pool. The substrate used for the deposition of coatings was pure aluminum (99.9%) and was sand blasted prior to the cladding experiments in order to clean the surface and obtain uniform roughness. The coatings were prepared by using the two-step cladding process. The optimized scan rate for cladding was 300 mm/min at a laser power of 5 kW. The optimization process has been reported elsewhere [9]. The subsequent remelting experiments were carried out employing scan rates of 300, 500, 1000 and 1200 mm/min. Characterization of the clad layers was performed using X-ray diffraction (JEOL JDX 8030) with $CuK_{\alpha} = 1.5402$ A, optical microscopy (using an Olympus microscope), scanning electron microscopy (JEOL JSM 840A), transmission electron microscopy (JEOL 2000FXII) and indentation hardness testing using a load of 25 gm (Shimadzu). At least five indents were made per location to obtain a good statistical representation of the dataset. In each case, the average of the five data was used to get the hardness plot for each track. The error bars represent the maxima and minima in each data set. The local phase composition was determined in SEM by standardless energy-dispersive X-ray analysis (EDX) on polished and etched sections. Numerous examinations of well equilibrated samples by point EDX in SEM have shown a scattering of the measured compositions in a range of 1 at.%. This scattering follows from the precision of the method rather than from compositional variation of the studied materials. Therefore, the precision of the compositional measurements presented in this paper is limited by ± 1 at.%. At least five independent measurements of the elemental composition of the different phases were made to get statistics of the compositional data.

3. Results

Fig. 1 shows the composite X-ray diffractograms of the clad and remelted samples. It is clear that the clad and remelted layers consist of a phase mixtures of the icosahedral phase (I), monoclinic $Al_{13}Fe_4(\lambda)$ and $CuAl_2(\alpha)$. The aluminum peaks are mainly due to the substrate. The peaks corresponding to I-phase are much more prominent in the case of the remelted tracks compared to the as-clad tracks.

Fig. 2 shows optical micrographs of both the clad and the remelted tracks. Fig. 2(a) shows a low magnification micrograph of the cross-section of the as-clad track revealing a dendritic growth morphology. The higher magnification micrograph (Fig. 2(b)) reveals all the phases present in the clad layers. The lath-shaped

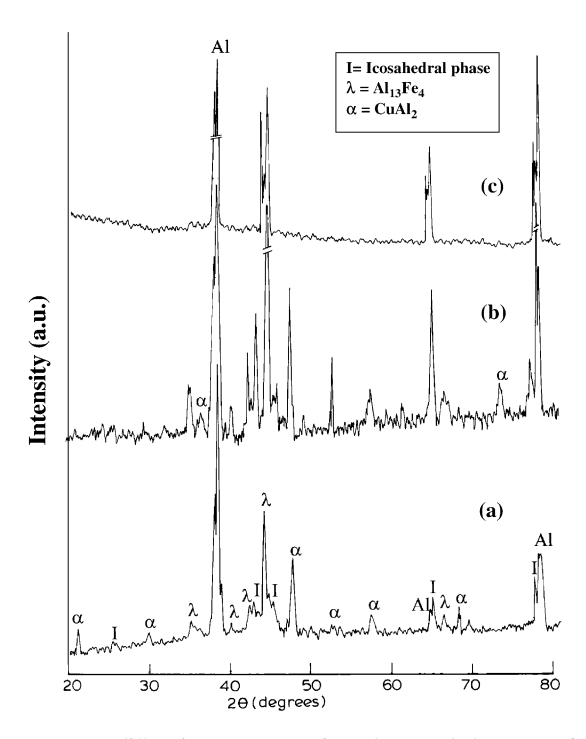


Fig. 1. X-ray diffraction patterns of tracks (a) clad 300 mm/min, (b) clad 300 mm/min and remelted mm/min and (c) clad 300 mm/min and remelted 500 mm/min.

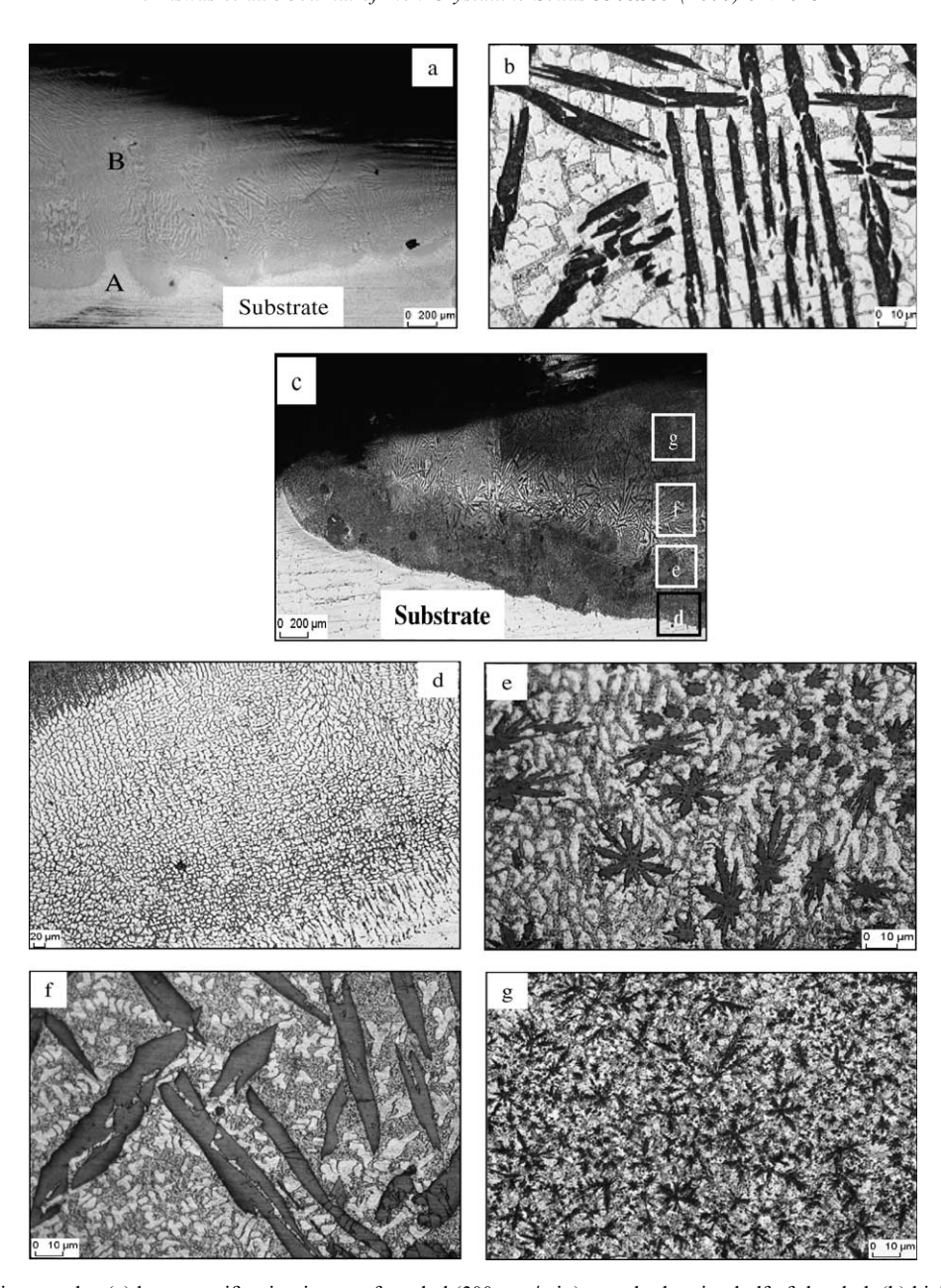


Fig. 2. The optical micrographs: (a) low magnification image of as-clad (300 mm/min) sample showing half of the clad, (b) high magnification image showing dendritic microstructure, (c) low magnification microstructure of remelted track (clad 300 mm/min and remelt 300 mm/min) showing different layers of microstructural features, (d)–(g) high magnification microstructures of the different regions marked in figure (c).

Al₁₃Fe₄ phase can be found throughout the clad. Fig. 2(c)–(g) show optical micrographs of the cross-section of the remelted track (remelted at 300 mm/min). The low magnification micrograph (Fig. 2(c)) reveals different layers across the height of the track. The high magnification micrographs of the various regions marked in Fig. 2(c) are shown separately. The interface between the clad and the substrate (Fig. 2(d)) shows a cellular morphology. A similar microstructure has also been observed in the case of the as-clad track near the substrate. Fig. 2(e) shows a high magnification microstructure of the region 'e' marked in Fig. 2(c). It shows

the formation of a dendrite with a ten-pointed star like morphology. The presence of ten-pointed stars is also detected in as-clad samples. Some of the stars are nearly perfect while others have some arms growing more than the other arms and have a distorted shape. The grain sizes of the nearly perfect stars vary between 5 and 20 µm. The perfect symmetry of the star would require a 36° angle between the adjacent points and the observed values are very close to that. Fig. 2(f) shows a high magnification microstructure of the region marked 'f' in Fig. 2(c). The microstructure is similar to that observed in Fig. 2(b) and it contains long, faceted dendrites

embedded in a two-phase matrix. The top layer or remelted layer (Fig. 2(g)) exhibits a significant reduction in the scale of microstructure. One can observe fine dendrites embedded in a finer, two-phase matrix.

Fig. 3 shows scanning electron micrographs taken from the remelted track. Fig. 3(a) shows a backscattered image (BSE) from a region similar to that shown in Fig. 2(e) showing ten-pointed stars. The inset shows a typical EDS profile taken from one of the stars. The composition analysis allows us to identify that these dendrites are $Al_{13}Fe_4$ ($Al_{74\pm2.5}Cu_{5\pm2}Fe_{21\pm2}$), consistent with X-ray diffraction results. The BSE image also shows the presence of a black phase; EDS analysis established this to be aluminum. Similarly, the fine white eutectic net-

work contains CuAl_2 ($\text{Cu}_{32\pm2}\text{Al}_{68\pm1.5}$) and aluminum. The BSE image taken from the region Fig. 2(f) is shown in Fig. 3(b). It clearly reveals three phases: lath-shaped $\text{Al}_{13}\text{Fe}_4$ (gray), blocky CuAl_2 and a eutectic consisting of aluminum and CuAl_2 . The inset shows a higher magnification of the area shown in the Fig. 3(b). The growth of an additional phase at the interface of the $\text{Al}_{13}\text{Fe}_4$ dendrite can be seen very clearly. The EDS analysis shows that the composition is $\text{Al}_{64\pm3}\text{Cu}_{22\pm2}\text{Fe}_{12\pm2}$, which is very close to the canonical composition of the icosahedral phase in Al-Cu-Fe system [10].

The transmission electron microscopic observations of the remelted sample (remelted at 300 mm/min) are presented in Figs. 4 and 5. Fig. 4(a) shows a typical low

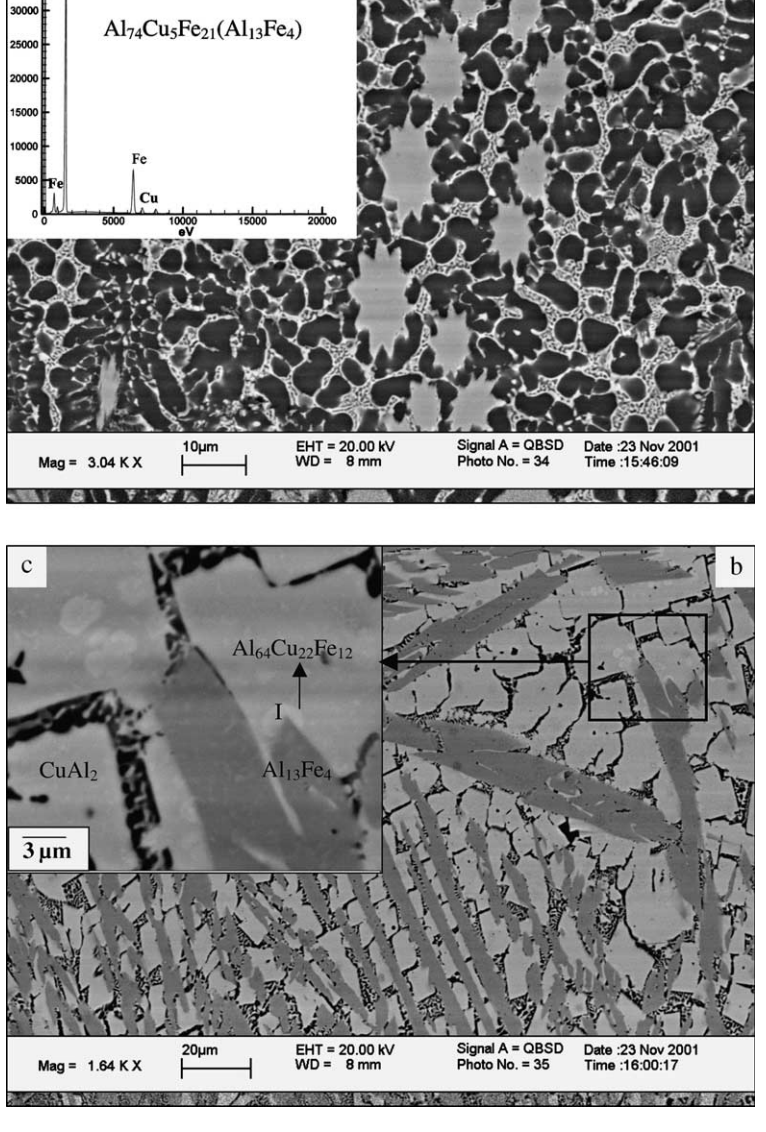


Fig. 3. Back scattered scanning electron micrographs (remelted 300 mm/min): (a) the layer corresponding to Fig. 2(e) showing ten-pointed star-like $Al_{13}Fe_4$ dendrites with the inset showing the EDS spectrum (b) layer corresponding to Fig. 2(f) showing lath-shaped $Al_{13}Fe_4$ along with the icosahedral and $CuAl_2$ phases and (c) the inset showing growth of the icosahedral phase by a peritectic reaction.

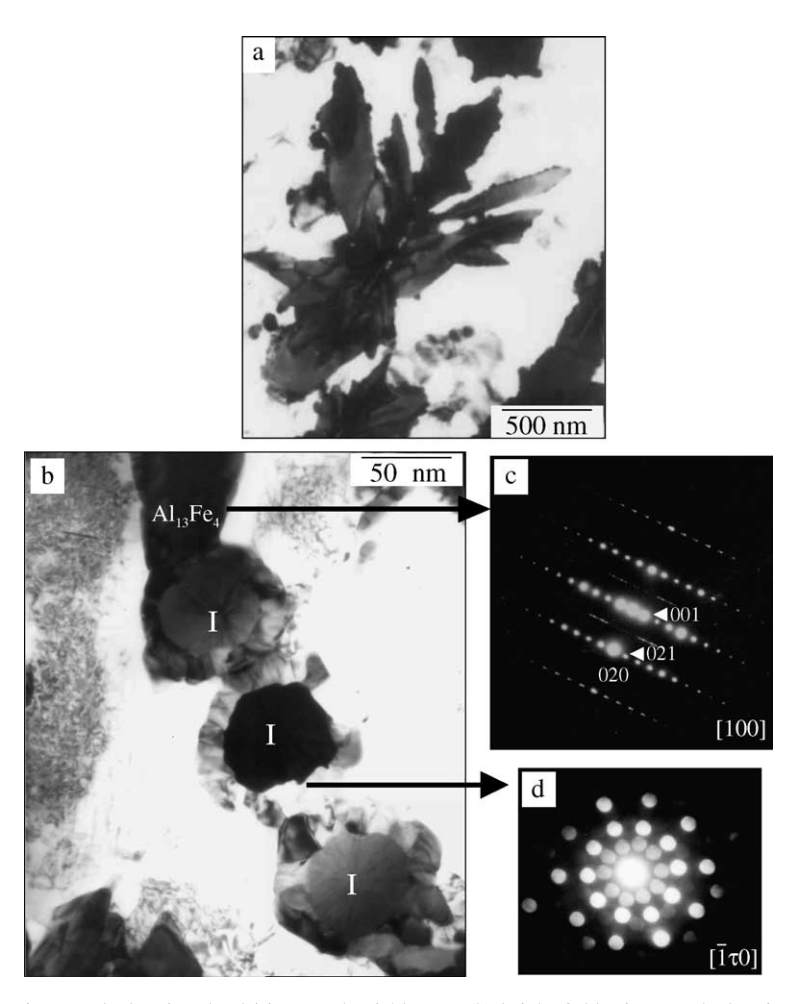


Fig. 4. (a) Typical bright field micrograph showing dendritic growth of $Al_{13}Fe_4$, (b) bright field micrograph showing the growth of the icosahedral phase at the interface of the $Al_{13}Fe_4$ dendrite, (c) [1 0 0] zone axis pattern of $Al_{13}Fe_4$, (d) microdiffraction pattern taken from one of the icosahedral phase particles showing a typical 5-fold diffraction pattern.

magnification bright field image of Al₁₃Fe₄ dendrites, which are faulted. The diffraction pattern taken along the [100] direction is shown in Fig. 4(c), which shows streaking and elongation of the spots. The growth of an icosahedral phase from the surface of an Al₁₃Fe₄ can be seen in Fig. 4(b), showing a bright field image that reveals the growth of a number of icosahedral phase particles. All of the icosahedral phase particles are not oriented in similar way. The microdiffraction pattern taken along [1 τ 0] from one of the particles is shown in Fig. 4(d). The independent growth of the icosahedral phase can also be observed in the sample. Fig. 5(a) shows a low magnification bright field image depicting such particles. The high magnification image Fig. 5(b) shows the typical mottled contrast of icosahedral phase particles. The corresponding microdiffraction patterns taken along different directions are shown in Fig. 5(c)-(e). Together, these patterns confirm the formation of icosahedral phase.

The hardness profiles of the clad and remelted tracks are shown in Fig. 6. It is clear that the level of hardness in all the tracks is quite high ($HV_{0.025} > 600$). The as-clad

track shows higher hardness ($HV_{0.025} > 750$) compared to the remelted tracks. In the case of the remelted tracks, the hardness values vary from place to place, whereas a steady hardness level is maintained throughout the whole clad layer in the as-clad track. Of all the remelted tracks, the track remelted at 300 mm/min shows the highest level of hardness.

4. Discussion

The present results indicate the feasibility of synthesizing quasicrystal containing composite coatings on a pure aluminum substrate by laser processing. The X-ray diffraction study indicates the presence of the icosahedral quasicrystalline phase, Al₁₃Fe₄, CuAl₂ and Al in the laser processed clad layers. The microstructure indicates two distinct zones, A and B (Fig. 2(a)). Zone B, which covers most of the regions, consists of a primary phase having a crystal structure similar to that reported for Al₁₃Fe₄ phase. The microstructure development indicates that the rest of the liquid is copper rich. The

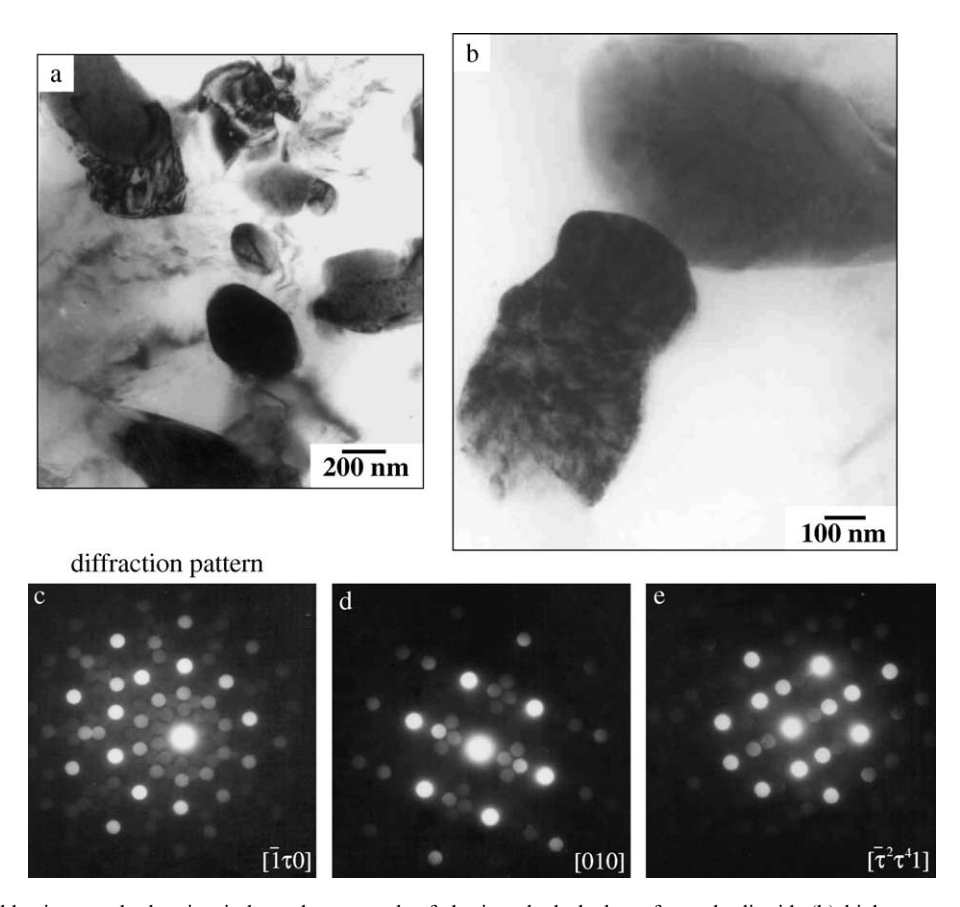


Fig. 5. (a) Bright field micrograph showing independent growth of the icosahedral phase from the liquid, (b) higher magnification micrograph showing mottled contrast, (c)–(e) show microdiffraction patterns taken from one such icosahedral phase particle.

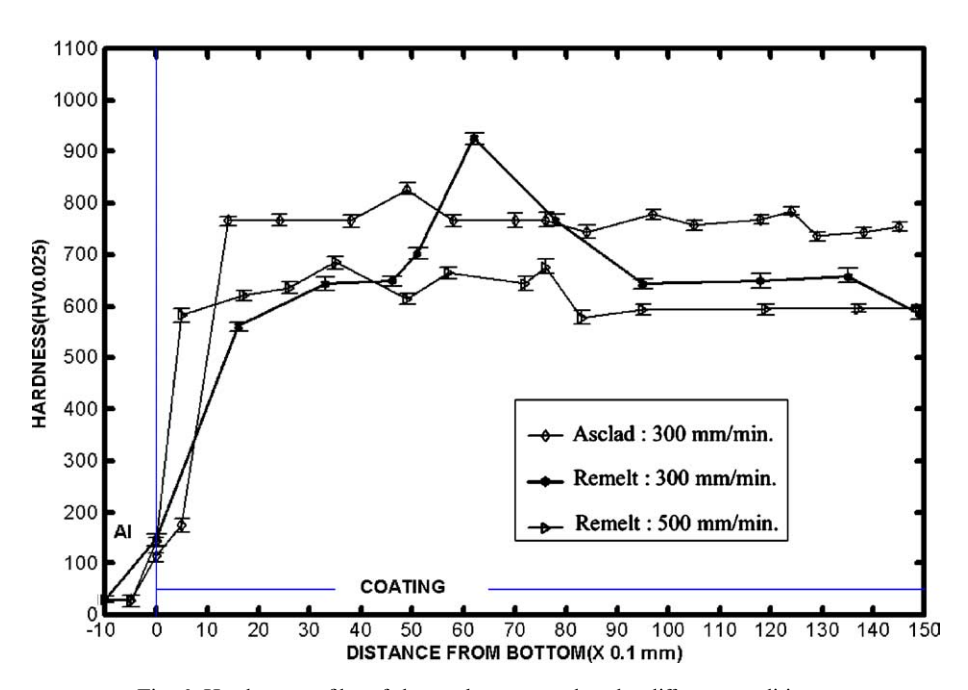


Fig. 6. Hardness profiles of the tracks processed under different conditions.

solidification of this copper-rich liquid yielded primary faceted CuAl₂ dendrites with an interdendritic region

consisting of the eutectic of α -Al and CuAl₂. Zone A consists of α -Al growing from the substrate with a cel-

lular morphology. The transition from zone A to zone B is sharp and probably triggered by heterogeneous nucleation of the $Al_{13}Fe_4$ phase on the growing α -Al liquid interface as the concentration of the alloying elements increased in the melt away from the substrate. The evolution of the microstructure in the remelted regions is more complex. Clearly the microstructure of the remelted zone at the top is finer. There is a significant increase in the fraction of the quasicrystalline phase in this region. We also observe the presence of the I-phase away from the Al₁₃Fe₄ dendrites. The I-phase generally forms by a peritectic reaction between Al₁₃Fe₄ and liquid in the present composition domain [11]. Only at a higher undercooling, can the I-phase form directly from the liquid. Thus, clearly the remelted liquid has undergone significant undercooling permitting direct nucleation of the I-phase. The middle layer (zone 'f' in Fig. 2(c)) is identical to zone B in the as-clad sample. This suggests that this layer is the remnant of the as-clad structure. Similarly, the microstructure of layer 'd' in the remelted sample is identical to the layer A of the as-clad sample. However, the presence of layer 'e' with a distinctly different microstructure indicates melting of the region near the aluminum substrate during remelting leading to the dilution of the clad layer by aluminum. The microstructure in region 'e' is significantly refined. Although the primary phase in the region is again Al₁₃Fe₄ dendrites, they are much finer, indicating that the region experienced a higher cooling rate during resolidification. The microstructure of the region in between the star-shaped dendrites is distinctly different in comparison to region 'f'. Here α-Al solidified as the primary phase in contrast to CuAl₂ phase (see Fig. 3(a)). This supports our conclusions of remelting and dilution by molten aluminum near the interface. Interestingly, the hardness of the clad layers is not significantly affected by these microstructural changes, suggesting that all the competing intermetallic phases, I-phase, Al₁₃Fe₄ and CuAl₂ may contribute in a similar manner to developing the hardness profile of the composite.

5. Conclusion

We have synthesized a composite coating of an Al-containing alloy consisting of quasicrystalline and related phases by laser cladding using an elemental powder mixture and subsequent remelting. A gradient microstructure develops in the remelted layer, which can be explained qualitatively by involving compositional changes and the solidification process during laser processing. The hardness of the coating is relatively insensitive to the microstructural change.

Acknowledgements

The authors would like to acknowledge the support of Indo-German co-operative programme of BMBF, Germany for carrying out this work.

References

- U. Köster, W. Liu, H. Hertzberg, M. Michel, J. Non-Cryst. Solid 153/154 (1993) 446.
- [2] S.S. Kang, J.M. Dubois, J. von Stebut, J. Mater. Res. 8 (10) (1993) 2471
- [3] S.-L. Chang, W.B. Chin, C.-M. Zhang, C.J. Jenks, P.A. Thiel, Surf. Sci. 337 (1995) 135.
- [4] J.M. Dubois, A. Proner, B. Bucaille, P. Cathonnet, C. Dong, V. Richard, A. Pianelli, Y. Massiani, S. Ait Yaazza, E. Belin-Ferré, Ann. Chim. Phys. 19 (1994) 3.
- [5] C.C. Homes, T. Timusk, X. Wu, Z. Altounian, A. Sahnoune, J.O. Strøm-Oslen, Phys. Rev. Lett. 13 (2) (1990) 129.
- [6] M. Dubois, S.S. Kang, A. Perrot, Mater. Sci. Eng. A 179&180 (1994) 122.
- [7] K. Urban, M. Feuerbacher, M. Wollgarten, MRS Bull. 22 (11) (1997) 65.
- [8] C. Friburg, B. Gruskho, J. Alloys Compd. 210 (1994) 149.
- [9] K. Chattopadhyay, K. Biswas, S. Bysakh, G. Phanikumar, A. Weishit, R. Galun, B.L. Mordike, MRS Proc. 643 (2001) K15.3.1.
- [10] A.P. Tsai, A. Inoue, T. Masumoto, Jpn. J. Appl. Phys. 26 (9) (1987) L1505.
- [11] S.M. Lee, H.J. Jeon, B.H. Kim, W.T. Kim, D.H. Kim, Mater. Sci. Eng. A 304–306 (2001) 871.